Permafrost, Phillips, Springman & Arenson (eds)

Modelling gelifluction processes: the significance of frost heave and slope gradient

C. Harris & J.S. Smith
Department of Earth Sciences, Cardiff University, Cardiff, United Kingdom

ABSTRACT: In this paper we describe laboratory modelling of gelifluction processes using the geotechnical centrifuge technique. Frozen 1/10 scale planar slope models were frozen from the surface downwards on the laboratory floor and thawed, also from the surface downwards, under gravitational acceleration of 10 gravities. A natural sandy silt soil formed the base test material and slope models at gradients 4°, 8°, 12° and 16° were. Each slope model was subjected to four cycles of freezing and thawing except for the 16° model, which failed during the first thaw cycle. During thaw, soil temperatures and pore water pressures were recorded continuously, together with soil thaw settlement and surface displacement. Following each experiment, models were sectioned to observe displacement columns embedded within the soil mass, which showed the profiles of soil movement and allowed volumetric displacements to be calculated. It is shown that both frost heave and slope gradient strongly affect rates of surface movement.

1 INTRODUCTION

This paper describes scaled centrifuge modelling of gelifluction processes. Gelifluction and frost creep are dominant in a wide range of arctic and alpine environments (e.g. Mackay 1981, Washburn 1967, 1999, Gorbunov & Seversky 1999, Matsuoka & Hirakawa 2000), and rates depend on many environmental factors, including slope gradient, soil moisture content, soil granulometry and vegetation (Pissart 1993, Matsuoka 2001). On natural slopes, spatial and temporal variability leads to complex multifactor controls on movement rates, demanding many site-specific studies with careful parameterisation of material properties and climatic inputs to arrive at detailed quantitative analyses (Washburn 1999). For this reason, laboratory simulation in which model boundary conditions and soil properties are precisely controlled, may provide new insights, both at full-scale (Harris et al. 1995, 1997) and, as here, in scaled experiments in which models are tested under an enhanced gravitational field in the geotechnical centrifuge (Harris et al. 2000a, b, 2001).

2 RESEARCH STRATEGY

Harris et al. (2000a, b, 2001) described centrifuge modelling of gelifluction and mudflow processes in a series of experiments using a natural silt-rich soil from Northern France. Here we report some initial results of an on-going project to investigate systematically the influence of (a) slope gradient, and (b) soil granulometry on thaw-related slow mass movement processes. The initial test soil consisted of the finer matrix material (<4 mm) from relict Quaternary periglacial mass movement deposits at Prawle Point, Devon, England (Table 1). It is hoped that results of this study will provide new evidence for precise mechanisms of Quaternary slope sediment accumulation in the test soil source area and allow estimates of likely timescales.

Table 1. Soil properties, Prawle test soil.

Clay (%)	Silt (%)	Sand (%)	LL (%)	PI (%)	ϕ'°	c'(kPa)
5	16	79	18	4	35	2

In the series of experiments discussed here, gelifluction was simulated on uniform planar slopes constructed of raw test soil at gradients of 4°, 8°, 12° and 16°.

3 SCALING ISSUES

Scaled model experiments must be based on similarity laws derived from fundamental equations governing the phenomena to be investigated (Higashi & Corte 1971). Since the stress/strain behavior of granular soils is non-linear, but a function of stress level and stress history, accurate scaled modelling requires that self-weight stress distribution within the model correctly replicates the prototype (Croce et al. 1985, Savvidou 1988). In a 1/N scale model tested on the laboratory floor (that is at 1 gravity (g)), self-weight stress at any depth below the surface is 1/N that at the equivalent depth in the full-scale prototype, and soil stress-strain behavior cannot be modelled accurately. However, stress similitude between model and prototype may be achieved by testing the scaled model in a geotechnical centrifuge with a gravitational field (centrifugal acceleration) equivalent to N times gravity (Harris et al. 2000a, b, 2001).

Mass movement rates in thawing ice-rich slopes are determined largely by effective stress conditions, so that pore water pressures play a critical role. The thaw consolidation theory (Morgenstern & Nixon 1971) provides an analytical framework for pore pressures, the governing factors being the rate of thaw penetration (controlling rate of release of melt-water) and the coefficient of consolidation (controlling rate of dissipation of excess pore water pressure):

$$R = \frac{1}{2}\left[\frac{\alpha}{\sqrt{c_v}}\right] \tag{1}$$

where

$$\alpha = \frac{X_t}{\sqrt{t}} \tag{2}$$

R is the Thaw Consolidation Ratio, c_v is the coefficient of consolidation, and X is the depth of thaw penetration in time t. Since in centrifuge experiments, time for seepage and time for heat transfer both scale as $1/N^2$ (Croce et al. 1985, Savvidou 1988), no scaling conflicts arise in modelling of the thaw consolidation process, and model time is reduced by a factor of N^2 compared with prototype time.

This, however, leads to a potential scaling conflict if the dynamic response of the thawing soil is a function of viscosity, since the time scaling factor for viscous flow is 1/1. Thus thaw consolidation time scales are reduced by $1/N^2$ in the model compared with the prototype, but flow would take place at the same rates in both. In a "modelling of models" experiment, Harris et al. (in press) have demonstrated the rates of gelifluction are accurately reproduced at three different scales (1:1, 1:10 and 1:30), and conclude that gelifluction is not a viscosity controlled process, but rather based on plastic deformation controlled by effective stress during thaw consolidation.

In the experiments reported here, soil freezing took place on the laboratory floor, and thawing at elevated gravity. It is assumed that where the dimensions of the ice lenses in the model are small (<0.5 mm), as was the case here, the fabric of the frozen prototype soil is replicated at centrifuge scale and that the stress-strain behaviour of both frozen and thawing soil will be the same in the model and the prototype. However, for a given heaving ratio, it should be noted that in a frozen prototype profile, the number of ice lenses would have probably been greater, and their average thickness proportionately less, than was the case within the equivalent scaled model profile.

4 EXPERIMENTAL DESIGN

These experiments followed identical protocols to those described by Harris et al. (2000a, b, 2001), and readers are referred to these papers for more detailed experimental descriptions. Planar slope models were constructed within a 750 mm long, 450 mm wide, 40 mm high polypropylene test box by placing a 70 mm thick layer of test soil (scaling to 0.7 m at 10 g) onto a sand base inclined at the required slope angle (Fig. 1). Soil was placed dry, and lightly compacted. The test box was tilted so that the slope surface was horizontal, then the soil was saturated from below by means of a constant-head water supply connected to the basal sand. During saturation, a water table was maintained at the soil surface. Following saturation, the water table was lowered to approximately 10 mm above the test soil-basal sand interface and the model was consolidated for 24 hours under a stress of 3.8 kN/m^2. This was equivalent to the self-weight of the soil at a model-scale depth of approximately 20 mm during centrifuge testing at 10 gravities (g), scaling to 200 mm depth at prototype scale.

Five Type K thermocouples and three Druck miniature pore pressure transducers (PDCR-81), filled with de-aired antifreeze solution to protect them when frozen, formed vertical sensor strings in two locations along a transect 150 mm from one side of the model. Transducers measured a maximum pressure of 350 mb (35 kPa) with combined non-linearity and hysteresis of ±0.2%. All cabling was brought through the soil on this side so that a 300 mm (scaling to 3 m at 10 g) wide strip of slope (2/3 of the model width), remained with no sensors or cables. All soil displacements were measured in this section.

15 plastic discs of diameter 10 mm were embedded in the soil surface in three downslope transects (Fig. 2)

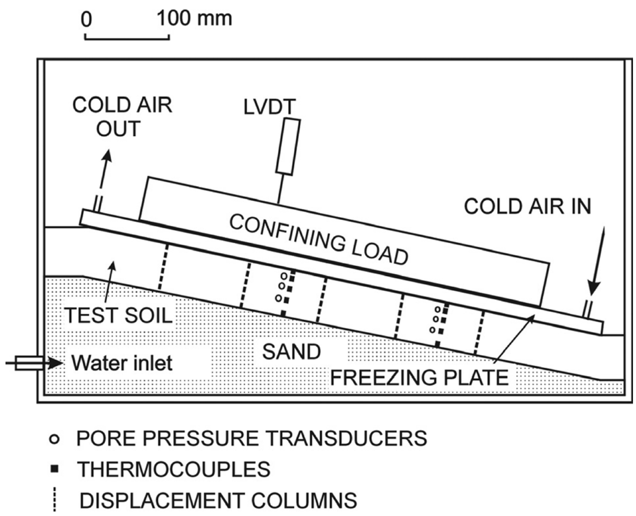

Figure 1. Experimental design for instrumentation and freezing of 1/10 scale slope models.

to measure surface displacement following each freeze-thaw cycle, and a total of 10 columns formed of plastic cylinders 5 mm in length and external diameter were installed to record downslope displacement profiles at the end of each test series. Columns formed two rows of five (Fig. 1), one down the centre line, the second 100 mm from the side of the model. The model container sides and base were first insulated and the model was then frozen from the surface downwards by means of a steel freezing plate placed on the slope surface. The plate temperature was lowered to −10°C using cold compressed air supplied from vortex tubes, and the test slope was frozen under a confining load of 3.8 kN/m^2. The phreatic surface was maintained in the base of the test soil during freezing, which lasted around 2 days. Surface frost heaving was measured manually along three slope profiles before and after freezing against a fixed datum.

Models were thawed in the centrifuge under a gravitational acceleration of 10 g. Thawing was from the surface downwards with air temperature maintained at approximately 20°C. During each thaw cycle, sensors were monitored at 30 s intervals via a Campbell Logger. The top surface and one side of the model were observed using miniature video cameras and frame grabbing from the resulting video tapes allowed movement of surface markers and thaw settlement to be monitored throughout each test to an accuracy of ±1 mm. All slope models were subjected to four cycles of freezing and thawing except that at 16° on which a mudflow began after the first thaw cycle. A summary of model parameters is given in Table 2.

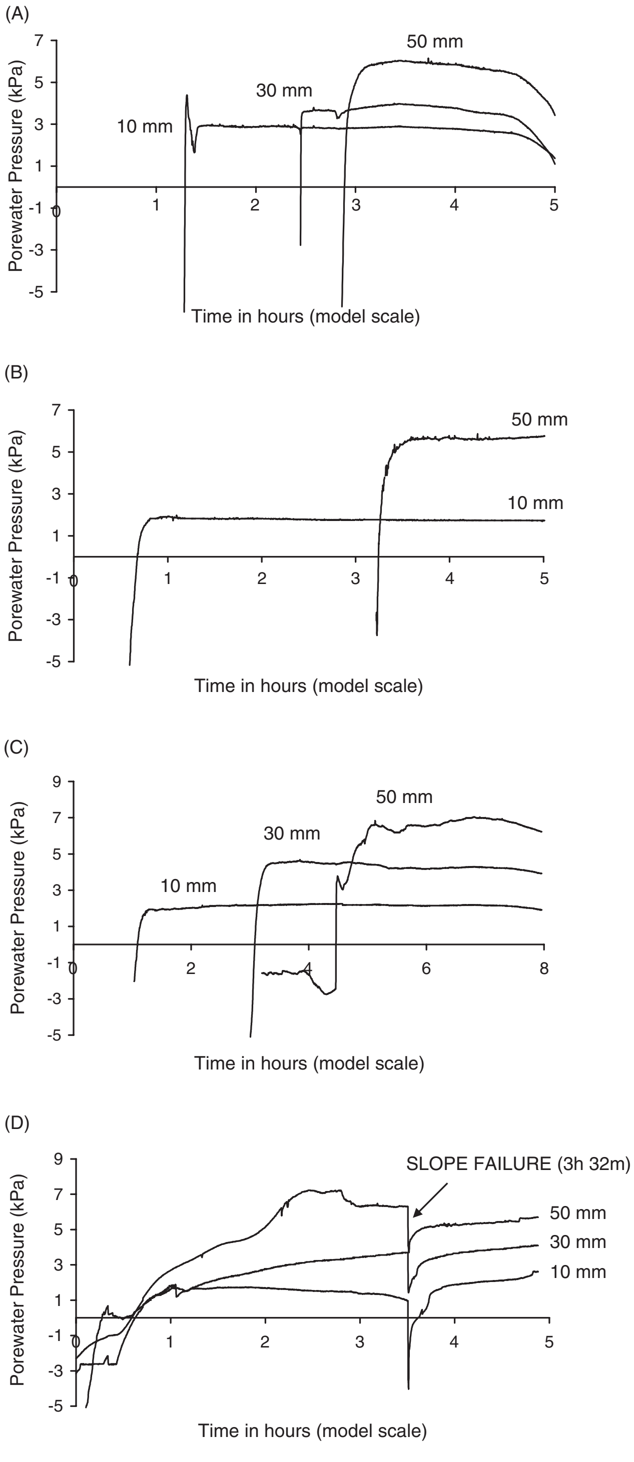

Figure 2. Examples of porewater pressure variations during thawing at 10 g in the centrifuge. (A) Test 1, cycle 1; (B) Test 2, cycle 1; (C) Test 3, cycle 2; (D) Test 4, cycle 1.

5 RESULTS

5.1 *Pore water pressures*

All tests showed a consistent style of pore water pressure change, with negative pore pressures recorded prior to thaw of the soil surrounding each transducer, but rapid rise to positive pressures following thaw (Fig. 2). This pattern is identical to that observed in full-scale simulation experiments using natural silt from Vire in Normandy (Harris et al. 1995, 1997, Harris & Davies 1998) and in later scaled centrifuge simulations using the same Vire silt (Harris et al. 2000, 2001a, b). The rise in pore pressure reflects release of meltwater into the soil and the initiation of thaw consolidation. As excess water is expelled from the thaw zone, and as consolidation proceeds, pore

Table 2. Model characteristics. Thaw rate is at prototype scale.

Test	Slope(°)	Number of cycles	Mean heaving ratio	Mean scaled thaw rate mm/day
1	4	4	0.15	25.6
2	8	4	0.14	28.5
3	12	4	0.17	31.0
4	16	1	0.18	32.4

pressures fall, though upward migration of water from the thaw zone maintains pore pressures in the near surface zones.

Factors of safety against slope failure were greater than unity for the first three test series, but in Test 4 (16°) pore pressures resulted in a flow slide slope failure. Back analysis indicated that the measured strength parameters (Table 1) slightly overestimate the cohesion value, with failure predicted with a cohesion parameter near 1.5 kPa. Note that the maximum recorded pore pressure at 50 mm model depth (scaling to 0.5 m prototype depth) prior to slope failure in Test 4 was 7.4 kPa (Fig. 2D), while hydrostatic pore pressure at 50 mm model depth was 4.9 kPa, and geostatic pressure approximately 9.07 kPa, so that recorded pore pressures were in excess of hydrostatic, but not approaching geostatic levels.

5.2 *Rates of surface movement*

Both displacement and thaw settlement of all surface markers was measured at the end of each thaw cycle to the nearest 0.25 mm. Surface displacement was strongly influenced by frost heave and thaw settlement. Some variation in frost heaving occurred between rows of surface markers in individual freezing cycles and slight variation was observed between cycles. Thus, average heave for each marker over the four cycles of freezing and thawing has been plotted against equivalent average downslope displacement (Fig. 3).

Although the mean heaving ratio (defined as the ratio of frost heave to frozen thickness of soil) and therefore thaw settlement differed slightly between successive tests (Table 2), a thaw settlement value of approximately 10 cm (prototype scale) falls approximately in the middle of the overall range (Fig. 3).

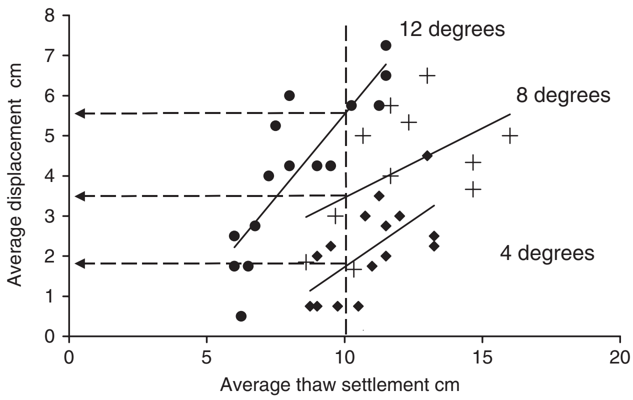

Figure 3. Relationship between average thaw settlement (cm) for each surface marker against average displacement per thaw cycle (cm). Predicted surface displacements arising from 10 cm thaw settlement are indicated for each slope model. Note, displacement and thaw settlement are quoted at prototype scale.

Using this value, mean surface displacements per cycle were determined, and plotted against the sine and tangent of the slope angles (proportional to the downslope shear stress, and potential downslope potential frost creep respectively), revealing linear relationships passing virtually through the origin (Fig. 4). If potential frost heave is taken as $h \cdot \tan\theta$ (Washburn

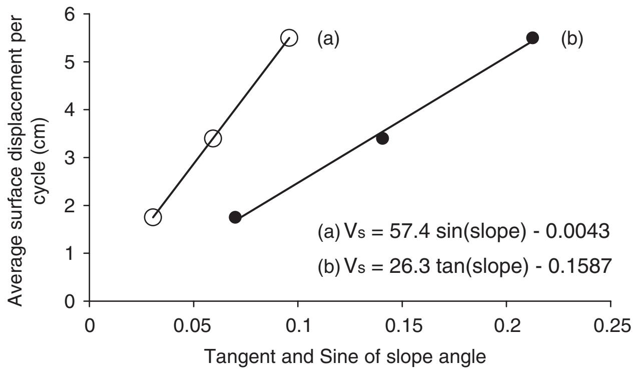

Figure 4. Relationship between mean surface displacement per cycle (at prototype scale) and (a) the sine of the slope angle, (b) the tangent of the slope angle.

(A) (B)

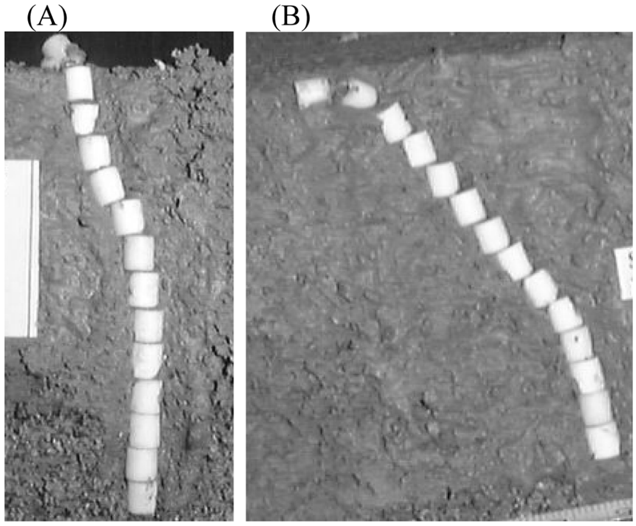

(C)

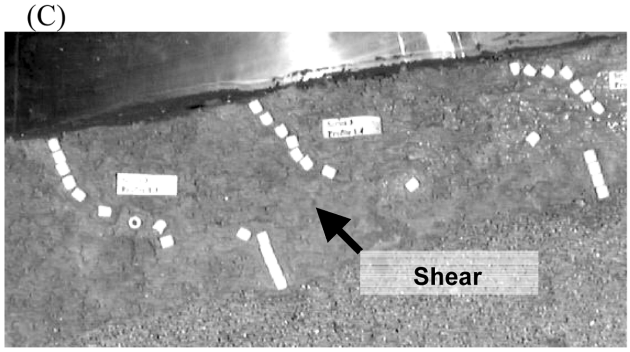

Figure 5. Profiles of movement: (A) Test Series 1 (4°) (B) Test Series 3 (12°) and (C) Test Series 4 (16°). Tests 1 and 3, four cycles of freezing and thawing, Test 4, failure during 1st thaw cycle.

1967), where h is heave/settlement and θ the slope angle, then potential frost creep makes up around 39% of the recorded movement, though actual frost creep was probably less than this.

5.3 *Sub-surface displacement profiles*

Volumetric transport rates may be determined from profiles of sub-surface movement, and these were measured at the end of each test series. Examples of observed profiles from Tests 1, 3, and 4 are shown in Figure 5. Due to technical problems, profiles are not available for Test 2. However, a second 8° gradient test series is currently in progress, and results will be used to analyse the influence of gradient on volumetric transport rates.

The profiles of movement revealed by excavation of Test Series 4 (16° slope gradient) show clearly the basal shear zone over which landsliding occurred.

6 DISCUSSION

Factors influencing rates of gelifluction have been discussed in a number of field studies, and recently summarised by Matsuoka (2001). Matsuoka emphasised the significance of frost heaving mechanisms, and recognised four typical displacement profiles (a) diurnal needle ice (rapid shallow surface displacement), (b) shallow diurnal ice segregation (slightly deeper and less rapid displacement), (c) annual one-sided active-layer freezing, (deeper, generally concave downslope profiles) and (d) annual two-sided active layer freezing (plug-like displacement of the active layer over an ice-rich basal shear zone). The experiments discussed here simulated one-sided annual active layer freezing, and generated profiles identical to category (c) of Matsuoka (2001). Profiles were also similar to earlier full-scale and scaled centrifuge simulations using Vire silt.

The complex interaction of factors, including frost heave, soil characteristics, soil thermal regime, slope gradient and vegetation, makes it extremely difficult to analyse the role of individual factors (e.g. Pissart 1993). Here we have concentrated on the significance of frost heave/thaw settlement and inclination, and demonstrated that for a given slope and active-layer thickness, surface movement rates are a direct function of frost heave/thaw settlement. This confirms earlier simulation experiments by Harris et al. (1995, 1997). Equally, for a given heaving ratio and hence thaw settlement, surface displacement rates are strongly correlated with the sine of the slope angle, which in turn determines shearing stress.

Matsuoka noted that “velocity varies widely with inclination within a study site” (Matsuoka 2001, p. 123), and this was certainly also true in these simulation experiments. He showed a wide range of surface velocities, but identified a maximum surface displacement rate where $V_s = 100 \tan\theta <$, where θ is the slope angle. The coefficient in these experiments was $\approx$26 (Fig. 4), suggesting that the modelling strategy (particularly soil type and thickness) adopted here has generated surface movement rates well below maximum, but representative of many of the sites included by Matsuoka.

Harris et al. (1995, 1997) demonstrated the critical importance of soil characteristics, since they affect frost susceptibility, permeability (and hence thaw consolidation ratio) and stress/strain relationships in the thawing soils Thus, the second stage in this research will concentrate on the effects of increasing silt and clay contents, and determination of corresponding geotechnical parameters. If modelling of sediment transport by periglacial mass movement (e.g. Etzelmüller et al. 2001) is to be calibrated and validated, analysis of as many contributing factors as possible is necessary, and this remains the long-term goal of this research.

7 CONCLUSIONS

1. Gelifluction associated with one-sided annual active layer freezing and thawing was successfully simulated.
2. For the silty sand test soil, the upper limit of the slope angle against mudsliding was close to 16° under the prevailing test conditions.
3. Rates of surface displacements due to gelifluction were strongly influenced by slope gradient and the amount of frost heave/thaw settlement.
4. For a given value of thaw settlement, surface velocity was very strongly correlated with the sine of the slope angle.
5. The simulated movement rates were comparable with results of many field studies.
6. Further research is in progress to investigate systematically the influence of soil properties.

ACKNOWLEDGEMENTS

This research was funded by the UK Natural Environment Research Council Research Grant GR3/12574. Technical support from Mr Ian Henderson is acknowledged.

REFERENCES

Croce, P., Pane, V., Znidarcic, H., Yo, H.Y., Olsen, H.W. & Schiffman, R.L. 1985. Evaluation of consolidation theories by centrifuge modelling. In W.H. Craig (ed.) *Application of Centrifuge Modelling to Geotechnical Design*: 381–401. Rotterdam: A.A. Balkema.

Etzelmüller, B., Ødegård, R., Berthling, I. & Sollid, J.L. 2001. Terrain parameters and remote sensing data in the analysis of permafrost distribution and periglacial processes: principles and examples from southern Norway. *Permafrost and Periglacal Processes* 12: 79–92.

Gorbunov, A.P. & Seversky, E.V. 1999. Solifluction in the mountains of Central Asia: distribution, morphology, processes. *Permafrost and Periglacial Processes* 12: 125–136.

Harris, C. & Davies, M.C.R. 1998. Porewater pressures recorded during laboratory freezing and thawing of a silt-rich soil. In *Proceedings 6th International Conference on Permafrost, Yellowknife, June 1998*: 433–440. Montreal: Laval University.

Harris, C., Davies, M.C.R. & Coutard, J.-P. 1995. Laboratory simulation of periglacial solifluction: significance of porewater pressure, moisture contents and undrained shear strength during thawing. *Permafrost and Periglacial Processes* 6: 293–312.

Harris, C., Davies, M.C.R. & Coutard, J.-P. 1997. Rates and processes of periglacial solifluction: an experimental approach. *Earth Surface Processes and Landforms* 22: 849–868.

Harris, C., Davies, M.C.R. & Rea, B. 2000a. Geotechnical centrifuge modelling of mass movement processes associated with thawing permafrost soils. *Landslides in research, theory and practice.* In E. Bromhead, N. Dixon & M.-L. Ibsen (eds) *Proc 8th International Landslide Conference*, *Cardiff*: 693–700. London: Thomas Telford.

Harris C., Davies, M.C.R. & Rea, B.R. 2000b. Geotechnical Centrifuge Modelling of Gelifluction: Validation of a New Approach to Cryogenic Mass Movement Process Studies. *Annals of Glaciology* 31: 417–421.

Harris, C., Rea, B. & Davies, M.C.R. 2001. Scaled physical modelling of mass movement processes on thawing slopes. *Permafrost and Periglacial Processes* 12: 125–136.

Harris, C., Davies, M.C.R. & Rea, B. (in press). Gelifluction: viscous flow or plastic creep? *Earth Surface Processes and Landforms*.

Higashi, A. & Corte, A.E. 1971. Solifluction: a model experiment. *Science* 171: 480–482.

Mackay, J.R. 1981. Active layer slope movement in a continuous permafrost environment, Gary Island, Northwest Territories, Canada. *Canadian Journal of Earth Sciences* 18: 166–1680.

Matsuoka, N. 2001. Solifluction rates, processes and landforms: a global review. *Earth-Science Reviews* 55: 107–134.

Matsuoka, N. & Hirahawa, K. 2000. Solifluction from one-sided and two-sided freezing: field data from Svalbard. *Polar Geoscience* 13: 187–201.

Morgenstern, N.R. & Nixon, J.F. 1971. One-dimensional consolidation of thawing soils. *Canadian Geotechnical Journal* 11: 447–469.

Pissart, A. 1993. Understanding the controls on solifluction movements in different environments: a methodology and its application in the French Alps. In B. Frenzel, B. (ed.) *Solifluction and Climatic Variation in the Holocene*: 209–215. Mainz: Akademie der Wissenschaften und der Literatur.

Savvidou, C. 1988. Centrifuge modelling of heat transfer in soil. *Centrifuge 88*: 583–591. Rotterdam: A.A. Balkema.

Washburn, A.L. 1967. *Instrumented observations of mass-wasting in Mesters Vig District, Northeast Greenlend*. Meddeleser om Grønland 166.

Washburn, A.L. 1999. A high arctic frost creep/gelifluction slope, 1981–89; Resolute Bay, Cornwallis Island, Northwest Territories, Canada. *Permafrost and Periglacial Processes* 10: 163–186.